An Approach to Identify Noise-Source Parameters of DC–DC Converter and Predict Conducted Emissions With Different Loads

Shuqi Zhang, Kengo Iokibe, *Member, IEEE*, and Yoshitaka Toyota, *Member, IEEE*

***Abstract*—The black-box equivalent-circuit model is generally used to predict electromagnetic interference (EMI) from dc–dc converters for assisting with filter design. We previously proposed a Norton-based two-port equivalent-circuit model excluding load to investigate the load effect on EMI. The EMI prediction presupposes constant internal impedances independent of the load change with only the noise current source change dependent on the load change. Under these conditions, the noise current source at any load can be calculated by using the numerical interpolation method. In this work, we used a dc–dc buck converter with a switching frequency of 200 kHz and identified the model parameters precisely by applying the waveform decomposition method. The internal admittances were found to be almost constant with respect to load change and only the input-port current source decreased with load. We then applied the cubic spline interpolation method to fit the input-port current source and calculate it at any load. This approach was verified by predicting the input-port noise voltage for loads between 3.3 and 15.6 Ω. Below 80 MHz, where the input-port current source decreased with load, the input-port voltage predicted using the input-port current source fitted by interpolation was in good agreement with the measured one.**

***Index Terms*—Conducted emission, cubic spline interpolation, dc–dc converter, equivalent circuit model, load effect, waveform decomposition.**

I. Introduction

THE BLACK-BOX model is widely used to predict electromagnetic interference (EMI) from electronic devices. This kind of model predicts EMI without looking into device details, which makes it suitable for complex circuits and system-level interference. The model generally consists of one or more pairs of Norton/Thevenin equivalent circuits for describing EMI behavior [1], [2], [3].

The modular terminal behavioral (MTB) model for characterizing switching module conducted emission was originally proposed in [1], and it has since been expanded into a generalized terminal model [2], [3]. However, the converter load is included and kept fixed in the terminal model, and the load effect on conducted emissions is unable to be addressed.

Manuscript received 31 May 2022; revised 13 November 2022; accepted 29 November 2022. Date of publication 9 December 2022; date of current version 23 March 2023. *(Corresponding author: Yoshitaka Toyota.)*

The authors are with the Graduate School of Natural Science and Technology, Okayama University, Okayama 700-8530, Japan (e-mail: pypl4x2y@s.okayama-u.ac.jp; toyota@okayama-u.ac.jp).

Digital Object Identifier 10.1109/LEMCPA.2022.3228199

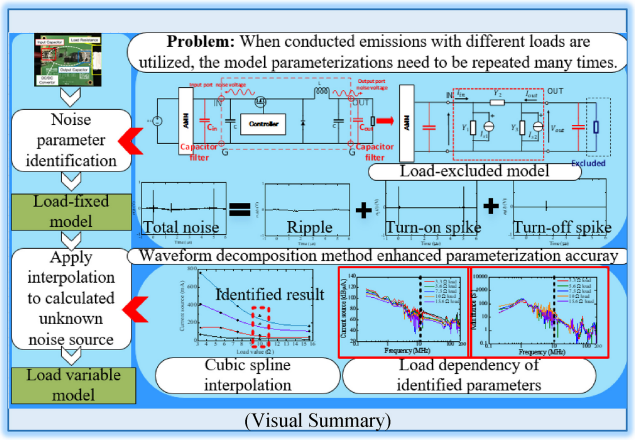

Several studies have examined the load effect on conducted emissions [4], [5]. Kostov et al. [4] investigated the conducted emissions from an SiC-based boost converter working under different conditions and found that the conducted emissions above 20 MHz increased with the load current. This indicates that the load is not independent of the EMI for the converter, which needs to be considered in the EMI modeling process. Yousaf et al. [5] suggested that the switching condition depends on load and investigated conducted emissions with various loads. They found that when the output load increased, the fundamental switching frequency and its harmonics were shifted to a higher frequency range because the internal operation condition changed with the load.

Take-Home Messages:

- As load is normally fixed in black-box EMI models, the parameterization process needs to be repeated many times. This letter proposes an approach to predict emissions from a DC-DC buck converter by using a black-box EMI model with different load values.
- The waveform decomposition method is applied to obtain the internal admittances and noise current sources precisely
- The results demonstrate that input port noise source is correlated with the load value, and several identified noise current sources can approximately predict unknown input port noise current sources of differential mode noise.
- The calculated input port noise source can be used to predict conducted emissions within a 5-dB error with any load value in a specific range.

Since the load affects the conducted emissions, the black-box model is expected to guide the filter design in different load cases. However, the generic black-box model can only be adapted to one specific load condition. Thus, a load-excluded black-box model is needed.

In our previous work [6], we proposed a load-excluded two-port equivalent-circuit model and subsequently conducted a preliminary study on the effect of load on equivalent noise parameters [7]. We were able to identify the noise parameters with several different loads and found that the internal impedances were independent of the load change and that only the noise current source was dependent on the load change. We also applied the linear interpolation method to predict the noise spectrum at an unknown load by using noise current source estimated from noise current sources identified at two different loads. However, we were unable to clarify the load effect on noise parameters because switching fluctuation affected the noise parameter identification in higher frequencies. In the current work, we apply the waveform decomposition method [8] to identify the model parameters precisely, along with a cubic spline interpolation method that is more accurate than the linear interpolation method.

In summary, in this letter, we propose a load-variable equivalent-circuit model to predict conducted emissions from various load values. The waveform decomposition method is applied to obtain the internal admittances and noise current sources precisely in Section II. The cubic spline interpolation method is then applied to fit the input-port noise current source in Section III. The evaluation results follow in Section IV.

II. Two-Port Equivalent Noise-Source Model and Load Effect on DC–DC Converter

In this section, we describe the parameter identification process in the black-box EMI model, where we apply the waveform decomposition method to remove the accuracy degradation by switching fluctuation and obtain accurate model parameters to verify the load effect.

A. Load Effect on DC–DC Converter Conducted Emission

We utilize a dc–dc buck converter (ROHM, BD9G341EFJ-EVK-101) operating at the switching frequency of 200 kHz for the model evaluation. The noise signal is measured in the time domain and converted into frequency spectra by fast Fourier transform (FFT) using MATLAB. The time-domain measurement can catch the noise magnitude and phase information at the same time, which is essential for black-box EMI modeling. An oscilloscope (Keysight DSOS104A) with three high-impedance passive 10:1 probes (KEYSIGHT N2894A, 700 MHz) with 1-MΩ input resistance and 9.5-pF input capacitance was used for measurement: 1) to measure the triggered signal from the switching node of the dc–dc converter and 2) to measure the input- and output-port signals. The input voltage was 18 V, and the output voltage was 5 V. The trigger was applied to the switching-node voltage. The measurement setup is shown in Fig. 1, where two probes are used for port noise measurement and one is used for measuring the switching node signal as a trigger source.

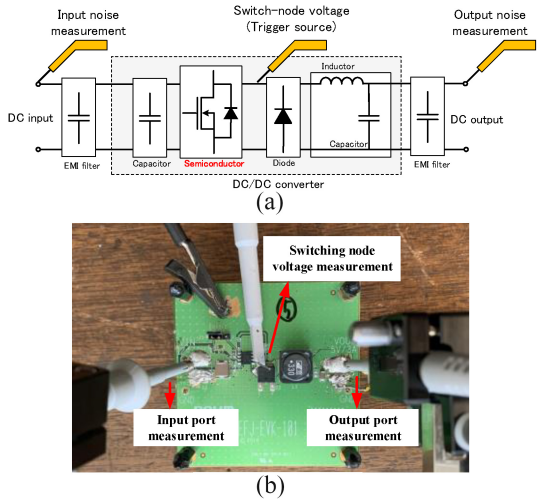

Fig. 1. Measurement setup. (a) Measurement schematic. (b) Testing view.

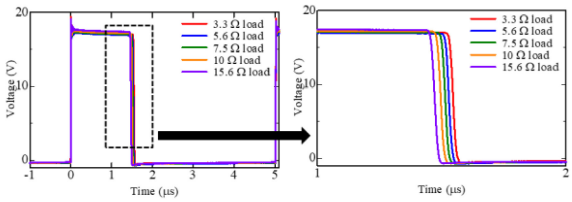

Fig. 2. Duty cycle with different loads.

In this letter, the dc–dc converter is working in the CCM, since if it works in the discontinuous condition mode (DCM), the diode needs to be turned off one more time, creating a third circuit condition. Moreover, the converter conducted emission with a heavy load in this letter is not rigorous.

Cement-filled fixed resistors (RGB10L-OHM-K) with a connector for changing loads easily were used for the evaluation. The parasitic inductance of the connector was 0.36 μH. Several loads are connected with the dc–dc converter, and the switching node voltage in Fig. 1 is observed with different loads. The measured results are shown in Fig. 2. The turn-on time is shorter with a larger load because the higher load current affects the feedback control process. Many studies on black-box EMI have set the load to fixed for the time-invariant system and included it in the model, the parameterization process has to repeat many times if the conducted emission is dealing with several different load conditions.

B. Waveform Decomposition Method

The waveform decomposition method [6] was utilized to avoid the effect of switching fluctuation. In this work, we set 10 MHz as the boundary between ripple noise and spike noise on the basis of preliminary observation indicating that the switching fluctuation does not affect low-frequency ripple noise below 10 MHz but does affect high-frequency spike noise above 10 MHz. Fig. 3 shows the schematic of noise waveform from the dc–dc converter in its original state and then decomposed into ripple noise, turn-on spike noise, and

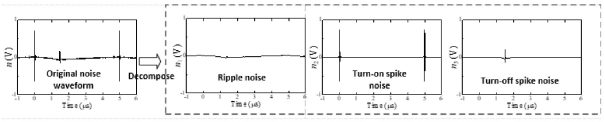

Fig. 3. Waveform decomposition applied to avoid switching fluctuation.

TABLE I
MEASUREMENT CONDITIONS

	Ripple noise	Turn-on spike noise
Sampling rate	1 Gs/s	10 Gs/s
Measurement time	250 μs	1 μs
Averaging times	1024	1024

turn-off spike noise. The following equation holds:

$$n(t) = n_1(t) + n_2(t) + n_3(t) \tag{1}$$

where $n_1(t)$ is the ripple noise, $n_2(t)$ is the turn-on spike noise, and $n_3(t)$ is the turn-off spike noise. The time-domain signal can be transformed into a frequency spectrum

$$N(f) = N_1(f) + N_2(f) + N_3(f) \tag{2}$$

where the frequency spectrum for each noise in one period can be obtained by FFT:

$$N_i(f) = FFT[n_i(t)] \quad (i = 1, 2, 3). \tag{3}$$

We measured the input-port and output-port noise with different loads and decomposed it into ripple noise and turn-on spike noise. The measurement conditions are listed in Table I.

For ripple noise, the measured time-domain noise signal is transferred to a frequency-domain spectrum by FFT and then a low-pass filter of the built-in function *designfilt* with a 10-MHz stopband is used to obtain the ripple noise in MATLAB. As for spike noise, we take turn-on spike as an example. The oscilloscope trigger is initially set to a rising slope and the triggered one-period signal is transferred to the frequency-domain spectrum. Next, we obtain the ripple noise spectrum by a low-pass filter and use IFFT to return the spectrum to the ripple signal and cut the ripple noise off in the time domain. We then obtain the ripple noise spectrum (below 10 MHz) and the spike noise spectrum (10–200 MHz). As for the turn-off spike noise, we set the trigger to a falling slope and the other processes are the same as the turn-on spike noise.

Although the turn-off spike noise has a similar trend to the turn-on spike noise, we do not show it in this letter due to the turn-off spike noise magnitude being lower in the 10–200 MHz range and overwhelmed by the turn-on spike noise. For easy visualization of noise over the entire frequency range, we combine the noise spectra into one unique spectrum in Fig. 4.

The measurement results show that a converter with a light load generates more input-port noise and a longer turn-on time. However, the output-port noise does not change significantly. The load current is high with a light load, and the increase in the load current also increases the maximum recovery current and thus the disturbance levels, as mentioned in [9]. These measurement results confirm that the noise amplitude

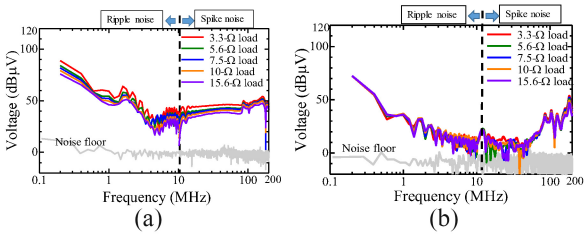

Fig. 4. Measured noise spectra with different loads. (a) Input-port recomposed spectrum. (b) Output-port recomposed spectrum.

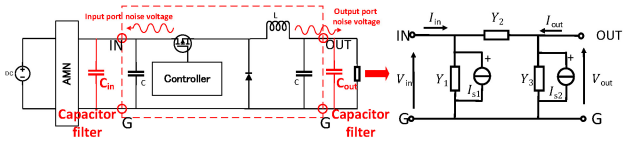

Fig. 5. Definition of two-port noise-source equivalent model.

is correlated with different loads. The input-port noise is our main interest here, as its magnitude changes with load value.

C. Model Definition and Noise Parameter Identification

Fig. 5 shows the two-port noise-source equivalent-circuit model we developed based on the Norton equivalent theorem [6]. The two-port model does not involve any system for CM noise prediction, and in our model, the load is excluded. Specifically, our two-port noise-source equivalent model focuses only on the normal mode because we want to investigate the load effect. Moreover, based on the study in [9], the CM noise does not significantly change with load, since the load only changes the power converter operating point and the gate resistance and the gate voltage of MOSFET remain stable. The circuit equations with the five noise parameters are derived from this noise model and are expressed as follows.

In [6], the circuit equations with the five model parameters $(\dot{Y}_1, \dot{Y}_2, \dot{Y}_3, \dot{I}_{s1}, \dot{I}_{s2})$ were derived from the noise model on the basis of Kirchhoff's current law and expressed as follows:

$$\begin{bmatrix} \dot{I}_{\text{in}} \\ \dot{I}_{\text{out}} \end{bmatrix} = \begin{bmatrix} \dot{V}_{\text{in}} & \dot{V}_{\text{in}} - \dot{V}_{\text{out}} & 0 & -1 & 0 \\ 0 & -(\dot{V}_{\text{in}} - \dot{V}_{\text{out}}) & \dot{V}_{\text{out}} & 0 & -1 \end{bmatrix} \begin{bmatrix} \dot{Y}_1 \\ \dot{Y}_2 \\ \dot{Y}_3 \\ \dot{I}_{s1} \\ \dot{I}_{s2} \end{bmatrix}. \tag{4}$$

To identify the model parameter, the input-port current, the input-port current $\dot{I}_{\text{in}}$ is calculated from input-port voltage $\dot{V}_{\text{in}}$ and the impedance of AMN. The output-port current $\dot{I}_{\text{out}}$ is calculated from input-port voltage $\dot{V}_{\text{out}}$ and load value. Accordingly, the conducted noise can be filtered by changing the capacitances at the input and output ports to obtain attenuated noise signals. The capacitor filter is used because it will affect neither the input dc voltage nor the duty cycle of the dc–dc converter. In this letter, we use a 4.7-μF X-capacitor with 5-mΩ ESR and 5-nH ESL (measured by the Keysight E5061B impedance analyzer) soldering in parallel for obtaining attenuated noise, which is the same as the condition in [8].

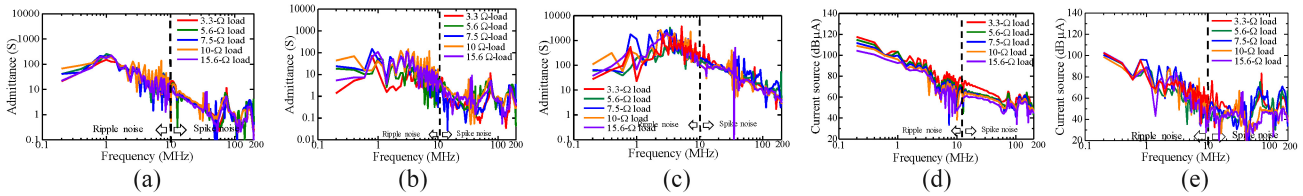

Fig. 6. Identified noise parameter magnitudes. (a) Y_1. (b) Y_2. (c) Y_3. (d) I_{s1}. (e) I_{s2}.

The filter conditions to obtain attenuated noise are 9.4 μF (two capacitors in parallel) and 18.8 μF (four capacitors in parallel). Besides, the cubic spline interpolation is used to calculate the noise parameters without the parameterization process.

III. Parameter Identification Results and Cubic Spline Interpolation Method for Variable Load Model

The identified parameters are shown in Fig. 6. To visualize the noise parameters in the entire frequency range, we combined the ripple noise parameter and turn-on spike noise parameter in the same figure. The turn-off spike noise is ignored because it is overwhelmed by the turn-on spike noise, as discussed earlier. The noise behavior parameters with different load values are indicated by different colors. The conducted emissions were measured and parameterized for five different load conditions.

The parameter identification results can be sorted into three parts: 1) input-port parameters I_{s1} and Y_1; 2) output-port parameters I_{s2} and Y_3; and 3) isolation admittance Y_2. Since the output-port noise changes only minimally with load, the load will not affect the noise parameter in the output port.

The input-port parameters are shown in Fig. 6(a) and (d). As we can see, the noise current source magnitudes I_{s1} are following the load value, and the noise admittance magnitudes Y_1 are independent of the load and show almost the same trend for each load. Errors occur at some frequencies because it is difficult to avoid errors in the least-squares method when solving (4), which is an overdetermined system.

Calculation errors tend to happen when fitting the results of unknown parameters. If the general trends of identified results are similar, we assume that the noise admittance magnitudes Y_1 are fixed. That is because the noise path on board does not change with load value like the result shown in Fig. 6(a).

The output-port parameters I_{s2} and Y_3 are shown in Fig. 6(c) and (e). Although errors occur in several frequencies, the trends of the noise current and noise admittance are assumed to be the same. As for the noise admittance magnitudes Y_2 shown in Fig. 6(b), the small load leads to a large noise current, which means that a larger isolation impedance is necessary. Thus, the smaller load value has smaller admittance magnitudes, which enables sufficient isolation between the input port and output port. Thus, if we could calculate the input-port current source I_{s1}, the input-port noise voltage with an unknown load is able to be predicted.

The noise source magnitude I_{s1} with load variations for different frequencies is shown in Fig. 7. For easy visualization,

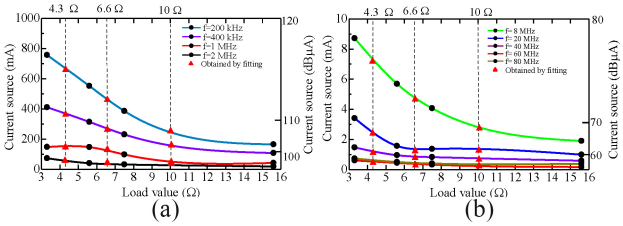

Fig. 7. Approximated curves of I_{s1}^{Rx} with load variation. (a) Below 2 MHz. (b) Between 8 and 80 MHz.

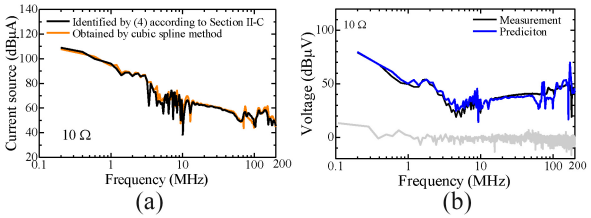

Fig. 8. Result evaluation with 10 Ω. (a) Comparison of $I_{s1}^{Rx=10\Omega}$ (b) Input-port noise voltage.

we separate the results into two parts: the noise source with higher magnitude (8–80 MHz) and lower magnitude (below 2 MHz), respectively. In Fig. 7, we can see that the identified noise source value decreases with increasing load value. With the consideration of interpolation accuracy and simplicity of calculation, we, therefore, propose the natural cubic spline interpolation method to approximate the I_{s1} without a parameter identification process as (5), where I_{s1}^{Rx} is the unknown current source with load value R_x [10]

$$I_{s1}{}^{\mathrm{Rx}} = \begin{cases} a_1R_x^3 + b_1R_x^2 + c_1R_x + d_1 & (3.3 \le R_x \le 5.6) \\ a_2R_x^3 + b_2R_x^2 + c_2R_x + d_2 & (5.6 \le R_x \le 7.5) \\ a_3R_x^3 + b_3R_x^2 + c_3R_x + d_3 & (7.5 \le R_x \le 15.6). \end{cases} \quad (5)$$

IV. Evaluation of Results

We used parameters with four different load values shown in Fig. 7 for evaluation of the results: 3.3, 5.6, 7.5, and 15.6 Ω, and noise current source with 10-Ω load is our prediction target. The noise parameters of four different loads were identified with the same process, i.e., only the load values were different.

The unknown current source $I_{s1}^{\mathrm{Rx}=10\ \Omega}$ at each frequency is calculated by (5) and is shown in Fig. 8(a). The noise current source identified by (4) according to Section II-C is the reference in black, and the orange curve shows the noise current source obtained from the cubic spline interpolation method. For input-port voltage prediction, we assumed

that noise impedances Y_1 and Y_3 are stable and Y_2 should be enough for isolation, so we used the other parameters of 3.3-Ω load with larger isolation admittance. The input-port voltage prediction result is shown in Fig. 8(b). We can see the prediction is in good agreement with the measurement.

In addition to the 10-Ω condition, we calculated other load values, such as 4.3 and 6.6 Ω in different load ranges of (5) and found that all the predictions showed good agreement with the measurements up to 80 MHz in the same way as 10 Ω though the figures are omitted due to space limitations. Above 80 MHz, since the load does not affect the input-port current source, we presume the deviation is caused by an accuracy degradation of the current source obtained by the numerical interpolation under the rank-deficient problem. Therefore, it is found that the proposed approach is valid as far as the input-port current source changes with load.

REFERENCES

[1] Q. Liu, F. Wang, and D. Boroyevich, "Modular-terminal-behavioral (MTB) model for characterizing switching module conducted EMI generation in converter systems," *IEEE Trans. Power Electron.*, vol. 21, no. 6, pp. 1804–1814, Nov. 2006.

[2] A. C. Baisden, D. Boroyevich, and F. Wang, "Generalized terminal modeling of electromagnetic interference," *IEEE Trans. Ind. Appl.*, vol. 46, no. 5, pp. 2068–2079, Sep./Oct. 2010.

[3] H. Bishnoi, A. C. Baisden, P. Mattavelli, and D. Boroyevich, "Analysis of EMI terminal modeling of switched power converters," *IEEE Trans. Power Electron.*, vol. 27, no. 9, pp. 3924–3933, Sep. 2012.

[4] K. Kostov, J. Rabkowski, and H.-P. Nee, "Conducted EMI from SiC BJT boost converter and its dependence on the output voltage, current, and heatsink connection," in *Proc. IEEE ECCE Asia Downunder*, 2013, pp. 1125–1130.

[5] J. Yousaf, M. Amin, S. Iqbal, H. Durrani, and M. K. Amin, "Conducted emission analysis of DC–DC converters and proper selection of pre-filtering stage," in *Proc. 10th Int. Bhurban Conf. Appl. Sci. Technol. (IBCAST)*, 2013, pp. 360–363.

[6] T. Uematsu, Y. Osaki, Y. Yano, K. Iokibe, and Y. Toyota, "Improvement of prediction accuracy of noise-source equivalent-circuit model based on parameter extraction by port voltage/current measurement," in *Proc. Joint Int. Symp. Electromagn. Compat. Asia–Pacific Int. Symp. Electromagn. Compat.*, 2019, p. 199.

[7] S. Zhang, T. Uematsu, K. Iokibe, and Y. Toyota, "Two-port noise source equivalent circuit model for DC/DC buck converter with consideration of load effect," in *Proc. Int. Symp. Electromagn. Compat. (EMC EUROPE)*, 2020, pp. 1–4.

[8] S. Zhang, T. Uematsu, K. Iokibe, and Y. Toyota, "Noise-source parameter identification considering switching fluctuation of DC–DC converter," in *Proc. IEEE Int. Joint EMC/SI/PI EMC Europe Symp.*, 2021, p. 186.

[9] M. Amara, C. Vollaire, M. Ali, and F. Costa, "Black box EMC modeling of a three phase inverter," in *Proc. Int. Symp. Electromagn. Compatibility (EMC EUROPE)*, 2018, pp. 642–647.

[10] M. Parviz, *Fundamentals of Engineering Numerical Analysis*, 2nd ed. Cambridge, U.K.: Cambridge Univ. Press, 2001, pp. 4–8.